JACS
JOURNAL OF THE AMERICAN CHEMICAL SOCIETY

Article

pubs.acs.org/JACS

Noninvasive and Reversible Cell Adhesion and Detachment via Single-Wavelength Near-Infrared Laser Mediated Photoisomerization

Wei Li,[†,‡] Zhaowei Chen,[†,‡] Li Zhou,[†,‡] Zhenhua Li,[†,‡] Jinsong Ren,*[,†] and Xiaogang Qu*[,†]

[†]Laboratory of Chemical Biology and State Key Laboratory of Rare Earth Resources Utilization, Changchun Institute of Applied Chemistry, Chinese Academy of Sciences, Changchun 130022, China

[‡]University of Chinese Academy of Sciences, Beijing 100039, China

Supporting Information

ABSTRACT: Dynamically regulating cell−molecule interactions is fundamental to a variety of biological and biomedical applications. Herein, for the first time, by utilizing spiropyran conjugated multishell upconversion nanoparticles (UCNPs) as a new generation of single-wavelength near-infrared (NIR)-controlled photoswitch, we report a simple yet versatile strategy for controlling cell adhesion/detachment reversibly and noninvasively. Specifically, the two-way isomerization of the photoswitch was merely dependent on the excitation power density of the 980 nm laser. At high power density, the ring-opening was prominent, whereas its reverse ring-closing process occurred upon irradiation by the same laser but with the lower power density. Such transformations made the interactions between spiropyran and cell surface protein fibronectin switchable, thus leading to reversible cell adhesion and detachment. Moreover, efficient adhesion-and-detachment of cells could be realized even after 10 cycles. Most importantly, the utilization of NIR not only showed little damage toward cells, but also improved penetration depth. Our work showed promising potential for in vivo dynamically manipulating cell−molecule interactions and biological process.

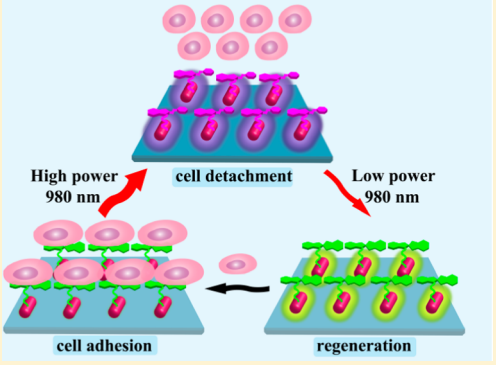

INTRODUCTION

Dynamically regulating the interactions between specific molecules and cell-surface molecules is critical for cell biology due to its potential to attain unprecedented levels of control over diverse cell behaviors even cell fate.[1] Especially, reversible control strategies, which enable real-time alternating such interactions between on−off states, have attracted particular attention since they can aid in the development of high-contrast optical bioimaging[2] and advanced therapies such as cell-based diagnostics[3] and immunotherapy.[4] For instance, reversible manipulation of polymeric materials and immune-cells interactions has been proposed to promote antitumor immunity.[4a] Although promising, the further cilnical application of these reversible methods was limited by the invasive and destructive implantable procedures. Thus, it still remains a big challenge to find an appropriate approach to regulate cell−molecule interactions facilely, reversibly, and noninvasively.

Among the various control strategies,[5] photomodulation has proven to be an ideal option by which cell−molecule interactions can be readily controlled with noninvasive property and high spatiotemporal precision.[5a−d] Particularly, photoswitching systems that undergo photoisomerization reactions have been used to reversibly guide cell-molecular recognition in interfacial systems.[6] Despite its usefulness, the photoswitches typically need to be modified with biomolecules, which requires complicated synthesis and even causes a distortion of the compounds.[7] An intriguing exception is the photochromic spiropyran. Unlike common photochromic systems, spiropyran itself with two different polar isomerizations has shown to be able to reversibly intercalate into DNA helix,[8] regulate enzyme activity,[9] and even specifically interact with cell surface protein fibronectin.[10] However, the need for two wavelength light-toxic ultraviolet and low penetrating visible light for ring-opening (350 nm) and ring-closing (560 nm) interconversion processes and the difficulties in focusing the two light beams precisely would complicate the practical process. Moreover, the inevitable cellular damage and poor tissue-penetration of the light used would limit their further biomedical applications. Recently, lanthanide-doped upconversion nanoparticles (UCNPs) have attracted much attention in nanobiotechnology due to their unique photophysical properties.[11] Generally, they can emit UV, visible, or near-infrared (NIR) light upon NIR excitation with a large anti-Stokes shift, which has been used to biologically friendly tune photoisomerization processes reported by our group[12] and others.[13] Especially, Branda and coworkers reported that the emission of an individual core−shell−shell UCNP can be modulated between UV and visible light by changing just the power intensity of one single 980 nm excitation light, which offered a simple way to regulate photochemical reactions.[14] Accordingly, by taking advantage of this unique feature, we envision that modulating the

Received: April 14, 2015
Published: May 28, 2015

DOI: 10.1021/jacs.5b03872
J. Am. Chem. Soc. 2015, 137, 8199−8205

Scheme 1. Schematic Illustration of the Utilization of SP-UCNP as a NIR-Triggered Photoswitch for Noninvasive and Reversible Control of Cell Adhesion/Detachment by Merely Altering the Power Density of a Single-Wavelength 980 nm Laser. At High Power (8 W/cm^2) Density, the UCNPs Can Emit UV Photons and Activate the Isomerization from the SP Form to the MC Form, Resulting in the Detachment of Cell. Conversely, When Exposed to Low Power (0.5 W/cm^2) Density, the Same UCNPs Can Emit Visible Light To Drive the MC Form Back to the SP Form, Leading to Cell Adhesion Again

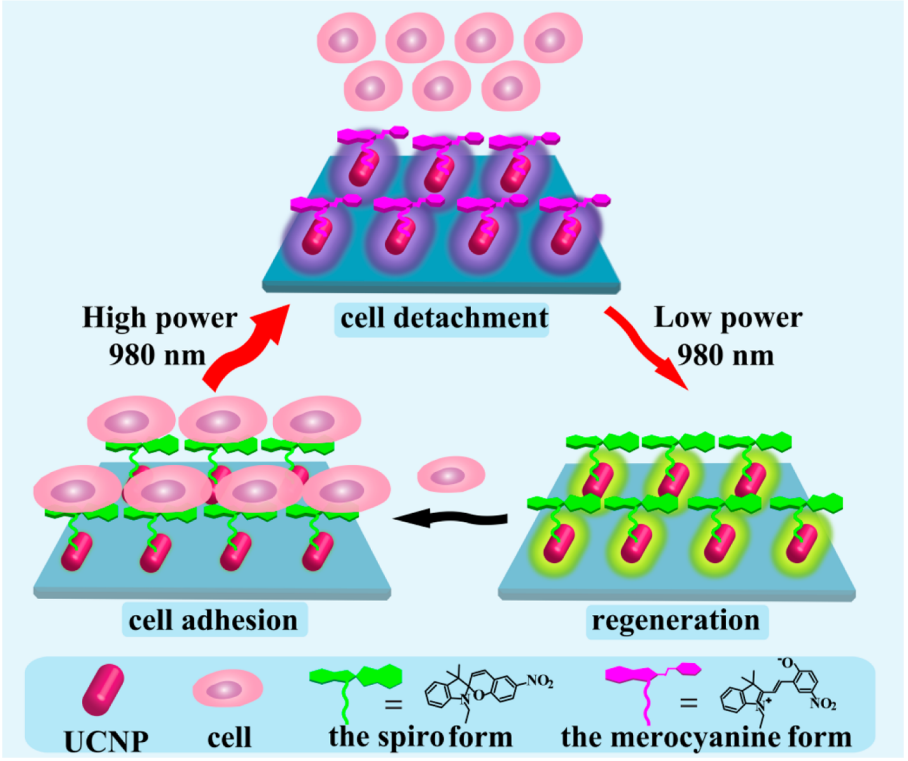

photochromic of spiropyran with this single-wavelength excited UCNP would provide a convenient but novel way to reversibly control the interactions between spiropyran and cells, which however has remained unexplored until now.

Herein, for the first time, by utilizing spiropyran conjugated multishell UCNP (SP-UCNP) as a new generation of single-wavelength NIR-controlled photoswitch, we report a simple yet versatile strategy for controlling cell adhesion/detachment reversibly and noninvasively. In this system, the isomerization of spiropyrans was merely dependent on the excitation power density of the 980 nm NIR laser (Scheme S1, Supporting Information). As illustrated in Scheme 1, at high power density, the UV emissions from UCNPs were prominent, and that, in turn, induced the formation of ring-opening merocyanine (MC) isomers. This isomerization process could be reversed by just reducing the power density to the point where the visible emission dominated. Such transformations made the interactions between spiropyran and cell surface protein fibronectin switchable, thus leading to reversible cell adhesion and detachment. Moreover, owing to the reversibility and the excellent photostability of the photoswitch, efficient adhesion-and-detachment of cells could be realized even after 10 cycles. Most importantly, the utilization of NIR not only showed little damage toward cells, but also improved penetration depth. We foresee that this new concept may hold great potential for biomedical application, especially for in vivo tissue engineering and medical implantation, etc.

RESULTS AND DISCUSSION

To minimize the energy loss induced by surface quenching effect,[15] we deposited a protecting layer of inert $NaYF_4$ onto the core−shell−shell UCNP[14,16] (layer-by-layer seed-mediated shell growth process and the enhanced luminescence intensity, for more details see the Supporting Information, Figures S1 and S2, respectively). Transmission electron microscopy (TEM, Figure 1a) demonstrated the as-designed core−shell−shell−shell UCNPs with an average size of 40 × 60 nm (width × length). The typical *d*-spacing value of 0.52 nm (high-resolution TEM, Figure 1b) and X-ray diffraction analysis (Figure S3) illustrated their single hexagonal-phase crystals. Subsequently, a 10 nm-thick (Figure 1c) silica shell was coated on the UCNPs by microemulsion method (UCNP@SiO_2),[12a] which enabled efficient energy transfer between spiropyran and UCNPs. Furthermore, energy dispersive spectroscopic (EDC) element mapping of Si, Y, Yb, Tm, and Er also verified the composition of the nanoparticles. After functionalized with (3-aminopropyl)-triethoxysilane (APTES), the resulting nanohybrids (UCNP@SiO_2−NH_2) were further covalently conjugated with carboxyl-containing spiropyran (SP-COOH, Scheme S2 and Figure S4). The surface modification processes (Scheme S3) were confirmed by Fourier transform infrared (FTIR, Figure S5) spectrum, and the typical aryl nitro stretching (1338, 1523 cm^{-1}) and acylamide vibration (1650 cm^{-1}) indicated the successful preparation of SP-UCNPs.

Next, we investigated the optical properties of SP-UCNP at high (8 W/cm^2) and low (0.5 W/cm^2) power densities of 980 nm NIR laser excitations. The maximum absorption peaks of the ring-closed spiro (SP) form located at 350 nm, which

DOI: 10.1021/jacs.5b03872
J. Am. Chem. Soc. 2015, 137, 8199−8205

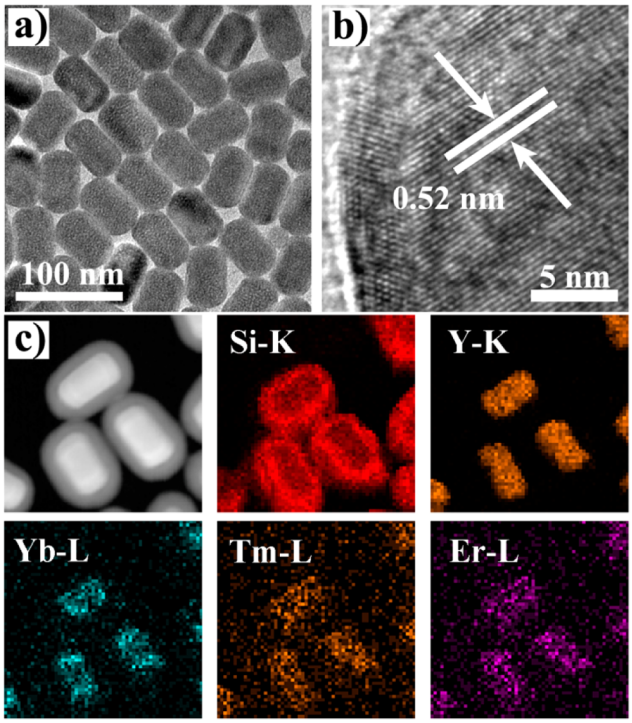

Figure 1. Structural characterization of the as-synthesized multishell UCNPs. (a) TEM image of $NaYF_4$:Tm/Yb@ $NaYF_4$@$NaYF_4$:Er/Yb@ $NaYF_4$ core−shell−shell−shell UCNPs. (b) High-resolution TEM image of a single UCNP. (c) Dark-field TEM image of UCNP@SiO_2 and corresponding EDC element mapping of Si K-edge, Y K-edge, Yb L-edge, Tm L-edge, and Er L-edge signals.

overlaps well with the UV emission of the UCNPs (attributed to $^1I_6 \rightarrow {}^3F_4$ (347 nm) and $^1D_2 \rightarrow {}^3H_6$ (365 nm) transitions of Tm^{3+} ions) under high power density excitation (Figure 2a).

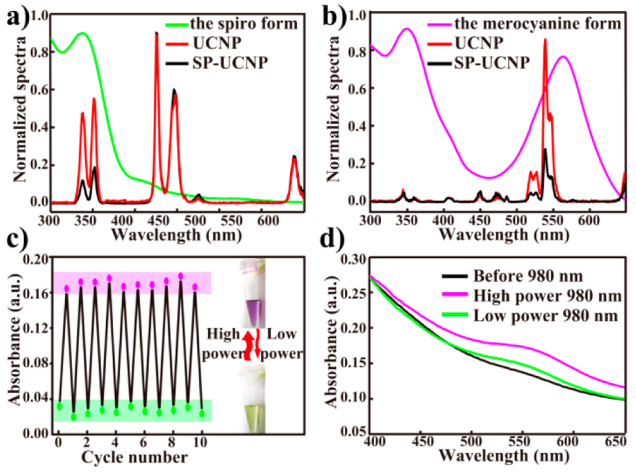

Figure 2. Optical characterization of the as-synthesized SP-UCNPs. (a) UV−vis absorption spectra of the SP form in DMF solvent and the UCL emission spectrum of UCNPs and SP-UCNPs under high power density (8 W/cm^2) of 980 nm NIR laser. (b) UV−vis absorption spectra of the MC form in DMF solvent, and the UCL emission spectrum of UCNPs and SP-UCNPs at lower power density (0.5 W/cm^2) of 980 nm NIR laser. (c) Irradiation cycles of SP-UCNPs; Inset: photographs of SP-UCNPs in DMF solvent under high power NIR and low power NIR, respectively. (d) UV−vis absorption spectra of SP-UCNPs modified surface before and subsequently irradiated with high/low power NIR laser.

This indicated that high power NIR excited UCNPs could be utilized to induce the ring-opening reaction of SP to MC through energy transfer process. The energy transfer process was verified by the significant quenching of upconversion fluorescence (UCL) emission around 350 nm, and the energy transfer efficiency was measured to be 75.76%. As illustrated in Figure S6, exposure of SP-UCNPs solution to high power density excitation resulted in an observable change in color from yellow to violet and a new band around 560 nm. The absorption strength increased over time and reached equilibrium within 6 min. Notably, merely reducing the excitation power density to 0.5 W/cm^2 would facilitate the overlap of the characteristic absorption of MC form at 560 nm and the visible emissions of the UCNPs generated from $^2H_{11/2} \rightarrow {}^4I_{15/2}$ (520 nm) and $^4S_{3/2} \rightarrow {}^4I_{15/2}$ (540 nm) transitions of Er^{3+} ions (Figure 2b), which could in turn be applied to trigger the reverse photoreactions. The energy transfer efficiency was calculated to be 68.8%, which certified the successful interconversion process. Additionally, the solution turned back to yellow, and the band at 560 nm disappeared upon being exposed to low power 980 nm irradiation for 10 min (Figure S7), which revealed the complete photoisomerization from MC to SP. The excitation-density-dependent UCL emission was attributed to the nonlinearity of the upconversion mechanisms, where higher excitation power density was needed to achieve a UV-emission-dominated spectral profile by first saturating other visible transitions.[17] These results clearly showed that the reversible two-way photoswitching of spiropyran could be driven by a single-wavelength NIR, and the direction of the photoisomerization could be modulated by merely increasing (for ring-opening) and decreasing (for ring-closing) the power density. The reversibility of the SP-UCNP photoswitch was tested by monitoring the absorbance at 560 nm while continuously alternating the power density between high/low (10 cycles). As shown in Figure 2, panel c and Figure S8, the photoisomerization with high/low NIR was reversible, and the efficiency of the switching was unaffected, confirming the robustness of SP-UCNP conjugation, which was mainly due to the attenuation of photofatigue by the utilization of noninvasive NIR.[18] Taken together, these results indicated that a new generation of photoswitch system was successfully built, which would facilitate the reversible control of cell adhesion/detachment.

In the following, we tested the photoswitching ability of SP-UCNP for regulating cell adhesion/detachment. First, we succeeded in fabricating the SP-UCNP modified surface by attaching UCNP@SiO_2−NH_2 to the amino group functionalized glass surface through glutaraldehyde and conjugating SP-COOH to the UCNPs with the grafting amount calculated to be 7.1 wt % (Scheme S4 and Figure S9). The SEM image revealed the uniform topography of the UCNP@SiO_2−NH_2 decorated surface (Figure S10), and the X-ray photoelectron spectroscopy (Figures S11 and S12) confirmed the successful procedure. As illustrated in UV−vis absorption spectra (Figure 2d), when exposure to 980 nm laser at high power density, the SP-UCNP modified surface exhibited an obvious enhancement band around 560 nm, certifying the ring-opening process. In contrast, the characteristic band disappeared after exposure to low power density of NIR, which ensured the effective ring-closing of spiropyran. The distinct change confirmed that the SP-UCNP on surface could be also effectively triggered by just modulating the power density of NIR laser, thus allowing the single-wavelength NIR mediated interfacial dynamic processes.

DOI: 10.1021/jacs.5b03872
J. Am. Chem. Soc. 2015, 137, 8199−8205

Afterward, we performed cell adhesion/detachment experiment via a single-wavelength NIR. Before cell adhesion, the modified surfaces were treated with different illuminations. Then HeLa cell suspensions (10^6 cells mL^{-1}) in a DMEM medium were incubated with the surfaces, and the amount of adhered cells was counted by a hemacytometer at varied time intervals (Figure 3a). Initially, the spiropyran were mainly in

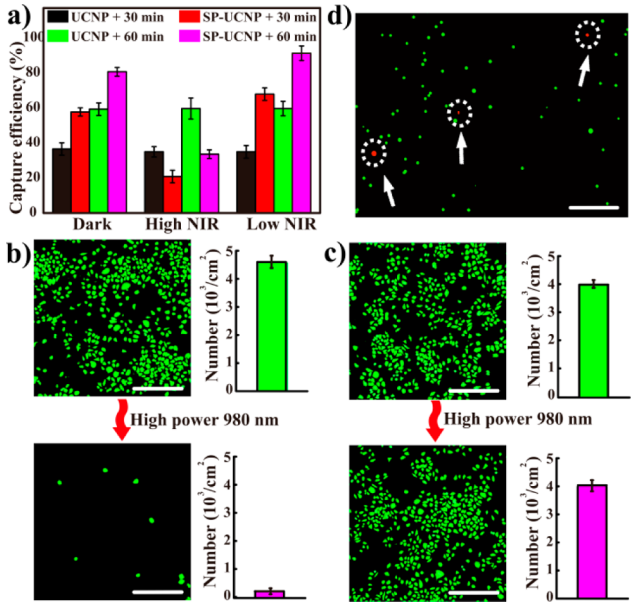

Figure 3. Single-wavelength 980 nm NIR regulates cell adhesion/detachment using the SP-UCNPs. (a) After treatment with different illuminations, cell capture efficiency of UCNPs modified surface and SP-UCNPs modified surface at varied time intervals was investigated. Fluorescence images of high power (8 W/cm^2) NIR induced cell detachment on (b) the system we designed and the system (c) without spiropyran. Scale bars are 100 μm. (d) Viability of released cell assessed with a live (green)/dead (red) assay.

the SP form, and the SP-UCNP modified surface demonstrated higher capture efficiency compared with the UCNP@SiO_2–NH_2 modified surface, which could be attributed to the specific interaction between SP isomerization and cell surface fibronectin protein.[10] Irradiation at high power density of 980 nm laser gave rise to the MC form, and a decrease in capture efficiency was observed, owing to the weak interaction between the MC form and fibronectin.[12a,19,20] Moreover, the low-power NIR illustrated surface displayed the highest capture efficiency among all the surfaces, further confirming that the SP-UCNP could be used as a new generation of photoswitch to guide cell adhesion. We then examined whether the utilization of a single-wavelength NIR could dynamically alter cell adhesion. After a 4 h incubation, the surfacewas gently washed with PBS, stained with calcein (AM) dyes, imagined, and counted under a microscope. As shown in Figure 3, panel b, over 95% original adherent cells were released from the SP-UCNPs based platform after exposure to high power 980 nm for 15 min (2.5 min break after 2.5 min irradiation to avoid heating effect of 980 nm laser). In contrast, no obvious detachment from the parallel surface (Figure 3c) was observed. These results confirmed that high power density of 980 nm laser could be applied to induce the photoisomerization in SP-UCNP photoswitch and further triggered the change of cell adherent behavior of the surface. Moreover, live/dead staining method (Figure 3d) was used to verify the good viability of cells released from the surface, which was necessary for practical cell culture and single cell analysis. In addition, the released cells remained functional and spread normally after recultured on the glass slide (Figure S13), which confirmed that the SP-UCNP based system could be used as an effective noninvasive cell adhesion/detachment platform for further biological investigations.

Another apparent advantage of the SP-UCNP based system is the ease of reversibly regulating cell adhesion/detachment on demand. By merely reducing the power density to 0.5 W/cm^2 and irradiating for 20 min, the surface could be reused for multiple cycles study. As demonstrated in Figure 4, panels a

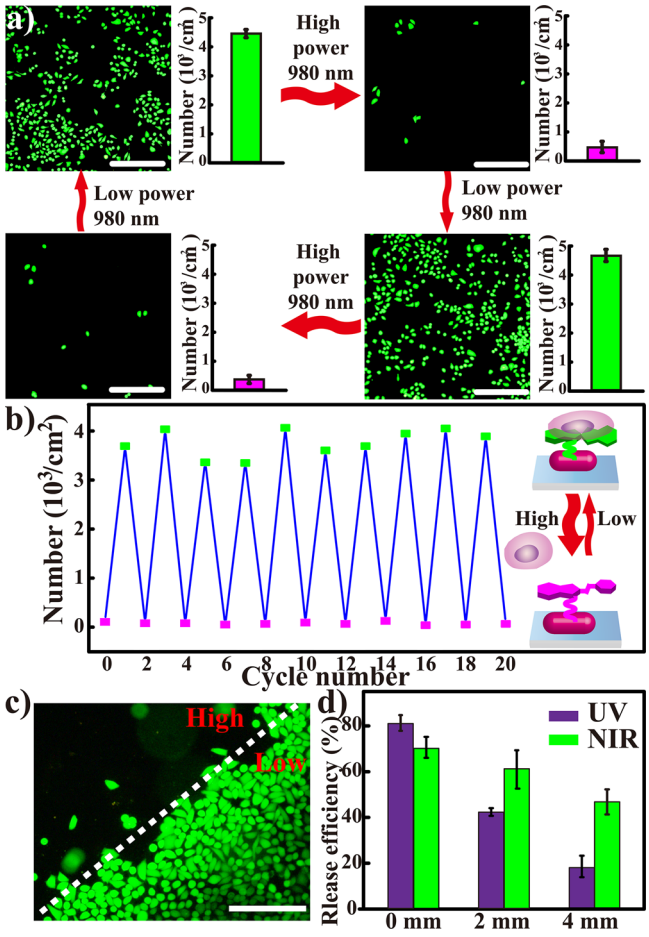

Figure 4. Single-wavelength 980 nm NIR regulates reversible control of cell adhesion and detachment. (a, b) Reversible adhesion and detachment of cells on SP-UCNPs modified system. Scale bars are 100 μm. (c) NIR-induced detachment of cells with pattern light irradiation. Scale bars are 100 μm. (d) Cell release efficiency induced by UV and NIR through 0, 2, or 4 mm of pork tissue.

and b and Figure S14, even after 10 cycles, the platform still showed high efficiency to cell detachment, which could be attributed to the outstanding reversibility and photostability of our NIR-triggered SP-UCNP photoswitch. Furthermore, the spatial control of cell adhesion was also demonstrated by alternating the power density between "high" and "low" site (Figure 4c), which provided an alternative method for cell patterning. Additionally, we investigated the feasibility of this system for application in deep tissues by using pork tissues as a model (Figure 4d, Scheme S5). As expected, only a slightly

DOI: 10.1021/jacs.5b03872
J. Am. Chem. Soc. 2015, 137, 8199–8205

reduced efficiency was observed for the NIR-triggered platform. In stark contrast, the cell release efficiency with UV irradiation decreased dramatically when it came to the tissue study, although direct exposure to UV showed a much higher efficiency than NIR. Importantly, the SP-UCNP decorated surface showed good reversibility even in tissue study (Figure S15). Taken together, these results verified that the utilization of NIR controlled SP-UCNP as a new generation of photoswitch not only greatly enhanced the reversibility of the platform and enabled spatial control of cell adhesion/detachment, but also significantly improved penetration depth.

CONCLUSION

In summary, for the first time, noninvasive and reversible regulation of cell−molecules interaction was successfully realized by utilizing spiropyran conjugated multishell UCNP as a single-wavelength NIR-controlled photoswitch. Notably, cell adhesion/detachment can be switched conveniently by merely decreasing/increasing the excitation power density of the same 980 nm laser, which greatly simplified the treatment process. Moreover, efficient adhesion-and-detachment of cells was achieved even after 10 cycles based on the reversible photoisomerization reactions and the excellent photostability of the photoswitch. Most importantly, the utilization of NIR not only showed little damage toward cells, but also significantly improved penetration depth, which is superior for further application. We anticipate that this single-wavelength NIR controlled approach would be further developed for in vivo dynamic control of biological process, tissue engineering, and medical implantation.

EXPERIMENTAL SECTION

Materials. All reagents and solvents were commercially available and used as received without further purification.

Synthesis of β-$NaYF_4$:Tm/Yb Core Nanoparticles. Briefly, 1.4 mmol $YCl_3{\cdot}6H_2O$, 0.6 mmol $YbCl_3{\cdot}6H_2O$, and 0.01 mmol $TmCl_3{\cdot}6H_2O$ were added to a 100 mL flask containing 12 mL of oleic acid and 30 mL of octadecene and heated to 160 °C to form a homogeneous solution. The temperature was then lowered to 50 °C, and the flask was placed under nitrogen gas protection. Once the reaction reached 50 °C, 10 mL of methanol solution containing NH_4F (296 mg, 8.0 mmol) and NaOH (200 mg, 5.0 mmol) was added in and kept under stirring for 30 min. After the methanol was slowly evaporated and the mixture was heated to 300 °C for 1.5 h under nitrogen protection, the solution was cooled down, and the resulting nanoparticles were purified by addition of ethanol, collected by centrifugation, and finally resuspended in 10 mL of cyclohexane.

Synthesis of $NaYF_4$:Tm/Yb@$NaYF_4$ Core−Shell Nanoparticles. A sample of 1.8 mmol $YCl_3{\cdot}6H_2O$ was added to a 100 mL flask containing 12 mL of oleic acid and 30 mL of octadecene and heated to 120 °C. The temperature was lowered to 80 °C, and the dispersion of $NaYF_4$:Tm/Yb core nanoparticles in hexanes was added. After the hexanes were slowly evaporated and heated to 110 °C, the mixture was cooled down to 50 °C. Once the temperature reached 50 °C, 10 mL of methanol solution containing NH_4F (259 mg, 7.0 mmol) and NaOH (175 mg, 4.4 mmol) was added in and kept under stirring for 30 min. After the methanol was slowly evaporated and the mixture was heated to 300 °C for 1.5 h under nitrogen protection, the solution was cooled down, and the resulting nanoparticles were purified by addition of ethanol, collected by centrifugation, and finally resuspended in 10 mL of cyclohexane.

Synthesis of $NaYF_4$:Tm/Yb@$NaYF_4$@$NaYF_4$:Er/Yb Core−Shell−Shell Nanoparticles. The same procedure outlined for the synthesis of core−shell $NaYF_4$:Tm/Yb@$NaYF_4$ was employed except that the core−shell nanoparticle was used as core, and $YCl_3{\cdot}6H_2O$ was used as precursor for epitaxial shell growth.

Synthesis of $NaYF_4$:Tm/Yb@$NaYF_4$@$NaYF_4$:Er/Yb@$NaYF_4$ Core−Shell−Shell−Shell Nanoparticles. The same procedure outlined for the synthesis of core−shell $NaYF_4$:Tm/Yb@$NaYF_4$ was employed except that the core−shell−shell nanoparticle was used as core, and $YCl_3{\cdot}6H_2O$ was used as precursor for epitaxial shell growth.

Synthesis of SP-COOH. During the synthesis, all the reaction vessels were wrapped in aluminum foil to ensure the reaction was performed in the dark. The preparation of the carboxy-containing spiropyran 1′-(β-carboxyethyl)-3′,3′-dimethyl-6-nitrospiro [indoline-2′,2-chromane] was performed as our reported paper.[12] In brief, 0.06 mol of 2, 3, 3-trimethylindole-nine, 0.06 mol of 3-iodopropanoic acid, and 5 mL of ethyl methyl ketone were refluxed under nitrogen at 100 °C for 3 h. The resulting mixture was dissolved in water, and the solution was washed with chloroform. After the evaporation of water, 1-(β-carboxyethyl)-2,3,3-trimethylindolenine iodide was achieved. Next, 0.04 mol of the resulting iodide, 0.04 mol of 5-nitrosalicylaldehyde, and 3.8 mL (0.04 mol) of piperidine were dissolved in ethyl methyl ketone and refluxed for 3 h. On standing overnight, a yellow crystalline powder was precipitated. The product was filtered and washed with methanol to yield SP-COOH (70% yield). The product was characterized by ^{1}HNMR spectroscopy as shown in Figure S1. ^{1}HNMR (400 MHz, $CDCl_3$, 25 °C, TMS): δ = 1.0−1.3 (6H; $2CH_3$), 2.6 (2H; CH_2COO), 3.4−3.5 (2H; CH_2N), 5.9−6.0 (2H; olefinic protons), 6.6−8.2 (aromatic protons).

Preparation of Silica-Coated UCNP. First, 7.2 mL of triton, 28 mL of cyclohexane, 7.2 mL of hexanol, 680 μL of water, and 50 mg of UCNPs were mixed in a 100 mL flask by sonication and agitation for 40 min. Then, 100 μL of TEOS was added dropwise into the mixture. Afterward, 160 μL of $NH_3{\cdot}H_2O$ was added into the flask and stirred for 24 h. The resulting nanoparticles were precipitated out by the addition of ethanol to yield UCNPs@SiO_2.

Preparation of Amino-Functionalized UCNP@SiO_2. Briefly, 20 mg of UCNPs@SiO_2 and 30 mL of toluene were first mixed in a 100 mL flask and heated to 110 °C. Next, 30 μL of APTES was added dropwise into the mixture. After being stirred for 24 h, the precipitates were separated by centrifugation, washed with ethanol three times, and dried at 60 °C for 12 h to obtain the UCNPs@SiO_2−NH_2.

Preparation of Spiropyran-Conjugated UCNP@SiO_2−NH_2. During the synthesis, all the reaction vessels were wrapped in aluminum foil to ensure the reaction was performed in the dark. A sample of 0.526 mmol of SP-COOH (200 mg) was first dissolved in 30 mL of dimethylformamide (DMF). Four milliliters of MES buffer (pH 6.0, 20 mM) containing EDC (500 mg) and NHS (400 mg) was added into the solution and agitated for 1.5 h. Afterward, 100 mg of UCNPs@SiO_2−NH_2 in 4 mL of MES buffer was added in and stirred for 48 h. The resulting nanoparticles were washed by water and DMF.

Preparation of the UCNPs Modified Substrate. The glass slide of 1 × 1 cm^2 was cleaned and immersed into 10 mL of 0.5% APTES solution for 1 h to introduce amino group. Then the amine-terminated substrates were reacted with the solution of UCNPs@SiO_2−NH_2 (10 mL/ml) for 24 h at room temperature.

Preparation of the SP-UCNPs Modified Surface. First, SP-COOH (200 mg, 0.526 mmol) was dissolved in 30 mL of DMF. Then EDC (500 mg) and NHS (400 mg) in 4 mL of MES buffer (pH 6.0, 20 nM) was added to the solution. After the solution was agitated overnight in the dark, the UCNPs modified surfaces were immersed into the solution for 24 h to conjugate with SP-COOH through EDC/NHS chemistry. The grafting amount of spiropyran on the UCNPs was calculated by UV−vis spectra.

NIR-Triggered Photoisomerization of the SP-UCNPs on Modified Surface. Before exposure to NIR illumination, the absorption spectra of the SP-UCNPs modified surfaces were recorded on JASCO V-550 UV−vis spectrophotometer. Subsequently, the surface was immersed in 500 μL of DMF and exposed to high power NIR irradiation for 5 min. The surfaces were dried out quickly before being measured. Afterward, the surface was immersed in 500 μL of DMF, exposed to low NIR irradiation for another 15 min, and measured again.

Cell Culture. The Hela cells were cultured at 37 °C in an atmosphere of 5% (v/v) CO_2 in Dulbecco's modified Eagle's medium

DOI: 10.1021/jacs.5b03872
J. Am. Chem. Soc. 2015, 137, 8199−8205

(DMEM) supplemented with 10% fetal bovine serum (FBS). The media was changed every 3 days, and the cells were digested by trypsin and resuspended in fresh complete medium before plating.

Cell Adhesion. The UCNP modified surface and SP-UCNP modified surface were pretreated with different illumination. Afterward, they were placed into a size-matched 24-well Lab-TekTM Chamber Slide. Hela cells were added to each culture flask to obtain a cell density of 1×10^6 cells per flask. The flasks were cultured in DMEM containing 10% FBS at 37 °C in an atmosphere of 5% CO_2. After being incubated for 30 min and 1 h, the surface was gently washed with PBS three times, and cell numbers in supernatant were counted by a hemacytometer again. The number of adhesion cells ($n_{adhesion}$) on the surfaces and the capture efficiency (e) can be calculated by the following equations, respectively:

$$n_{adhesion} = n_{total} - n_{supernatant}$$

$$e = n_{adhesion}/n_{total}$$

NIR Controlled Cell Detachment. After being incubated with cells for 4 h, the platform was examined for NIR triggered release. After irradiation NIR laser at the power density of 8 W/cm^2 for 15 min (2.5 min break after 2.5 min of irradiation to avoid heating effect of 980 nm laser), the surface was gently washed with PBS for 15 s to remove the released cells. Fluorescent microscopic imaging was used to monitor the cell release. For live/dead cell staining, the released cell was collected from the washing buffer by centrifugation at 1000 rpm for 5 min, and then propidium iodide (PI) and calcein (AM) dyes were added into the released cell. After 15 min of incubation, the cells were imaged by the microscope. For repeatability of the study, the substrates first were digested by trypsin and washed with PBS three times. Then the substrates were exposed to NIR at the powers of 0.5 W/cm^2 for 20 min and reused for cell adhesion and detachment. Furthermore, to control cell detachment regionally, we first treated the SP-UCNP modified surfaces with a dose of 20 min of lower power NIR illuminations and then incubated them with cells. Afterward, we shielded the surfaces with a light-proof photomask on one-half and put the surfaces under high power density NIR for 15 min. As the light source and photomask were removed, the surfaces were washed gently with PBS and recorded with microscope. For deep tissue irradiation, pork tissues (muscle tissue) with 0 mm, 2 mm, and 4 mm thickness were placed above the cell adhesive surface with a distance of 1 mm. The laser was irradiated from the top of the tissue.

Fluorescent Microscopic Imaging. For the imaging test, the surface was placed into 24-well plates and incubated with a density of 1×10^6 cells/well for 4 h at 37 °C in an atmosphere of 5% CO_2. AM dyes were added into the flask for 15 min. Then the substrates were gently washed with PBS and finally imaged under an Olympus BX-51 optical equipped with a CCD camera. After NIR irradiation, the substrates were gently washed with PBS, stained with AM for 15 min, and viewed under the microscope.

■ ASSOCIATED CONTENT

Ⓢ Supporting Information

Detailed experimental procedures and supplementary figures and tables. The Supporting Information is available free of charge on the ACS Publications website at DOI: 10.1021/jacs.5b03872.

■ AUTHOR INFORMATION

Corresponding Authors

*jren@ciac.ac.cn
*xqu@ciac.ac.cn

Notes

The authors declare no competing financial interest.

■ ACKNOWLEDGMENTS

We thank Wen Li from University of Chinese Academy of Sciences for the helpful advice on the manuscript. Financial support was provided by the National Basic Research Program of China (Grant Nos. 2012CB720602, 2011CB936004) and the National Natural Science Foundation of China (Grant Nos. 91213302, 21210002, 21431007, 91413111).

■ REFERENCES

(1) (a) Hynes, R. O. *Science* **2009**, *326*, 1216. (b) Herbert, S. P.; Stainier, D. Y. R. *Nat. Rev. Mol. Cell Biol.* **2011**, *12*, 551. (c) Robertus, J.; Browne, W. R.; Feringa, B. L. *Chem. Soc. Rev.* **2010**, *39*, 354. (d) Stevens, M. M.; George, J. H. *Science* **2005**, *310*, 1135.

(2) (a) Kim, Y.; Jung, H.-y.; Choe, Y. H.; Lee, C.; Ko, S.-K.; Koun, S.; Choi, Y.; Chung, B. H.; Park, B. C.; Huh, T.-L.; Shin, I.; Kim, E. *Angew. Chem., Int. Ed.* **2012**, *51*, 2878. (b) Takahashi, S.; Piao, W.; Matsumura, Y.; Komatsu, T.; Ueno, T.; Terai, T.; Kamachi, T.; Kohno, M.; Nagano, T.; Hanaoka, K. *J. Am. Chem. Soc.* **2012**, *134*, 19588.

(3) Liu, Q.; Wu, C.; Cai, H.; Hu, N.; Zhou, J.; Wang, P. *Chem. Rev.* **2014**, *114*, 6423.

(4) (a) Ali, O. A.; Huebsch, N.; Cao, L.; Dranoff, G.; Mooney, D. J. *Nat. Mater.* **2009**, *8*, 151. (b) Kim, J.; Li, W. A.; Choi, Y.; Lewin, S. A.; Verbeke, C. S.; Dranoff, G.; Mooney, D. J. *Nat. Biotechnol.* **2015**, *33*, 64. (c) Okano, F.; Merad, M.; Furumoto, K.; Engleman, E. G. *J. Immunol.* **2005**, *174*, 2645.

(5) (a) Lee, T. T.; García, J. R.; Paez, J. I.; Singh, A.; Phelps, E. A.; Weis, S.; Shafiq, Z.; Shekaran, A.; del Campo, A.; García, A. J. *Nat. Mater.* **2015**, *14*, 352. (b) Li, W.; Wang, J.; Ren, J.; Qu, X. *Angew. Chem., Int. Ed.* **2013**, *52*, 6726. (c) Li, W.; Wang, J.; Ren, J.; Qu, X. *J. Am. Chem. Soc.* **2014**, *136*, 2248. (d) Liu, D.; Xie, Y.; Shao, H.; Jiang, X. *Angew. Chem., Int. Ed.* **2009**, *48*, 4406. (e) Hou, S.; Zhao, H.; Zhao, L.; Shen, Q.; Wei, K. S.; Suh, D. Y.; Nakao, A.; Garcia, M. A.; Song, M.; Lee, T.; Xiong, B.; Luo, S.-C.; Tseng, H.-R.; Yu, H.-H. *Adv. Mater.* **2013**, *25*, 1547. (f) Liu, H.; Li, Y.; Sun, K.; Fan, J.; Zhang, P.; Meng, J.; Wang, S.; Jiang, L. *J. Am. Chem. Soc.* **2013**, *135*, 7603. (g) Zhang, P.; Chen, L.; Xu, T.; Liu, H.; Liu, X.; Meng, J.; Yang, G.; Jiang, L.; Wang, S. *Adv. Mater.* **2013**, *25*, 3566. (h) Zhang, Z.; Chen, N.; Li, S.; Battig, M. R.; Wang, Y. *J. Am. Chem. Soc.* **2012**, *134*, 15716.

(6) Weber, T.; Chandrasekaran, V.; Stamer, I.; Thygesen, M. B.; Terfort, A.; Lindhorst, T. K. *Angew. Chem., Int. Ed.* **2014**, *53*, 14583.

(7) (a) Schönberger, M.; Trauner, D. *Angew. Chem., Int. Ed.* **2014**, *53*, 3264. (b) Zhang, J.; Zou, Q.; Tian, H. *Adv. Mater.* **2013**, *25*, 378.

(8) Andersson, J.; Li, S.; Lincoln, P.; Andréasson, J. *J. Am. Chem. Soc.* **2008**, *130*, 11836.

(9) Song, Y.; Xu, C.; Wei, W.; Ren, J.; Qu, X. *Chem. Commun.* **2011**, *47*, 9083.

(10) (a) Higuchi, A.; Hamamura, A.; Shindo, Y.; Kitamura, H.; Yoon, B. O.; Mori, T.; Uyama, T.; Umezawa, A. *Biomacromolecules* **2004**, *5*, 1770. (b) Wang, N.; Li, Y.; Zhang, Y.; Liao, Y.; Liu, W. *Langmuir* **2014**, *30*, 11823. (c) Edahiro, J.-I.; Sumaru, K.; Tada, Y.; Ohi, K.; Takagi, T.; Kameda, M.; Shinbo, T.; Kanamori, T.; Yoshimi, Y. *Biomacromolecules* **2005**, *6*, 970.

(11) (a) Cheng, L.; Yang, K.; Li, Y.; Chen, J.; Wang, C.; Shao, M.; Lee, S.-T.; Liu, Z. *Angew. Chem., Int. Ed.* **2011**, *50*, 7385. (b) Huang, P.; Zheng, W.; Zhou, S.; Tu, D.; Chen, Z.; Zhu, H.; Li, R.; Ma, E.; Huang, M.; Chen, X. *Angew. Chem., Int. Ed.* **2014**, *53*, 1252. (c) Liu, J.; Liu, Y.; Liu, Q.; Li, C.; Sun, L.; Li, F. *J. Am. Chem. Soc.* **2011**, *133*, 15276. (d) Liu, Y.; Chen, M.; Cao, T.; Sun, Y.; Li, C.; Liu, Q.; Yang, T.; Yao, L.; Feng, W.; Li, F. *J. Am. Chem. Soc.* **2013**, *135*, 9869. (e) Yang, Y.; Shao, Q.; Deng, R.; Wang, C.; Teng, X.; Cheng, K.; Cheng, Z.; Huang, L.; Liu, Z.; Liu, X.; Xing, B. *Angew. Chem., Int. Ed.* **2012**, *51*, 3125. (f) Liu, J.; Liu, Y.; Bu, W.; Sun, Y.; Sun, Y.; Du, J.; Shi, J. *J. Am. Chem. Soc.* **2014**, *136*, 9701.

(12) (a) Chen, Z.; Zhou, L.; Bing, W.; Zhang, Z.; Li, Z.; Ren, J.; Qu, X. *J. Am. Chem. Soc.* **2014**, *136*, 7498. (b) Zhou, L.; Chen, Z.; Dong, K.; Yin, M.; Ren, J.; Qu, X. *Adv. Mater.* **2014**, *26*, 2424.

(13) (a) Lai, J.; Zhang, Y.; Pasquale, N.; Lee, K.-B. *Angew. Chem., Int. Ed.* **2014**, *53*, 14419. (b) Min, Y.; Li, J.; Liu, F.; Yeow, E. K. L.; Xing, B.

DOI: 10.1021/jacs.5b03872
J. Am. Chem. Soc. 2015, 137, 8199−8205

Angew. Chem., Int. Ed. **2014**, *53*, 1012. (c) Wang, L.; Dong, H.; Li, Y.; Xue, C.; Sun, L.-D.; Yan, C.-H.; Li, Q. *J. Am. Chem. Soc.* **2014**, *136*, 4480. (d) Zhang, B. F.; Frigoli, M.; Angiuli, F.; Vetrone, F.; Capobianco, J. A. *Chem. Commun.* **2012**, *48*, 7244. (e) Zhang, C.; Xu, C.-H.; Sun, L.-D.; Yan, C.-H. *Chem.—Asian J.* **2012**, *7*, 2225. (f) Liu, J.; Bu, W.; Shi, J. *Angew. Chem., Int. Ed.* **2013**, *52*, 4375. (g) Yang, T.; Liu, Q.; Li, J.; Pu, S.; Yang, P.; Li, F. *RSC Adv.* **2014**, *4*, 15613. (h) Boyer, J.-C.; Carling, C.-J.; Chua, S. Y.; Wilson, D.; Johnsen, B.; Baillie, D.; Branda, N. R. *Chem.—Eur. J.* **2012**, *18*, 3122.

(14) Boyer, J.-C.; Carling, C.-J.; Gates, B. D.; Branda, N. R. *J. Am. Chem. Soc.* **2010**, *132*, 15766.

(15) (a) Han, S.; Deng, R.; Xie, X.; Liu, X. *Angew. Chem., Int. Ed.* **2014**, *53*, 11702. (b) Peng, J.; Xu, W.; Teoh, C. L.; Han, S.; Kim, B.; Samanta, A.; Er, J. C.; Wang, L.; Yuan, L.; Liu, X.; Chang, Y.-T. *J. Am. Chem. Soc.* **2015**, *137*, 2336.

(16) (a) Wang, F.; Deng, R.; Wang, J.; Wang, Q.; Han, Y.; Zhu, H.; Chen, X.; Liu, X. *Nat. Mater.* **2011**, *10*, 968. (b) Wen, H.; Zhu, H.; Chen, X.; Hung, T. F.; Wang, B.; Zhu, G.; Yu, S. F.; Wang, F. *Angew. Chem., Int. Ed.* **2013**, *52*, 13419.

(17) (a) Pollnau, M.; Gamelin, D. R.; Lüthi, S. R.; Güdel, H. U.; Hehlen, M. P. *Phys. Rev. B* **2000**, *61*, 3337. (b) Shen, J.; Chen, G.; Ohulchanskyy, T. Y.; Kesseli, S. J.; Buchholz, S.; Li, Z.; Prasad, P. N.; Han, G. *Small* **2013**, *9*, 3213.

(18) Tong, R.; Hemmati, H. D.; Langer, R.; Kohane, D. S. *J. Am. Chem. Soc.* **2012**, *134*, 8848.

(19) Gelmi, A.; Zanoni, M.; Higgins, M. J.; Gambhir, S.; Officer, D. L.; Diamond, D.; Wallace, G. G. *J. Mater. Chem. B* **2013**, *1*, 2162.

(20) Bergkvist, M.; Carlsson, J.; Oscarsson, S. *J. Biomed. Mater. Res. Part A* **2003**, *64A*, 349.

■ NOTE ADDED AFTER ASAP PUBLICATION

Figure 4 was corrected on June 16, 2015.

DOI: 10.1021/jacs.5b03872
J. Am. Chem. Soc. 2015, 137, 8199−8205